Development of a Membrane-anchored Chemerin Receptor Agonist as a Novel Modulator of Allergic Airway Inflammation and Neuropathic Pain*

Jamie R. Doyle[‡], **Subrahmanian T. Krishnaji**[§], **Guangli Zhu**[¶], **Zhen-Zhong Xu**[‖**], **Daniel Heller**[‡], **Ru-Rong Ji**[‖**], **Bruce D. Levy**[¶], **Krishna Kumar**[§], and **Alan S. Kopin**[‡1]

From the [‡]Molecular Pharmacology Research Center, and Molecular Cardiology Research Institute, Tufts Medical Center, Boston, Massachusetts 02111, the [§]Department of Chemistry, Tufts University, Medford, Massachusetts 02155, the [¶]Department of Pulmonary and Critical Care Medicine, Brigham and Women's Hospital, Harvard Medical School, Boston, Massachusetts 02115, and the Departments of [‖]Anesthesiology and [**]Neurobiology, Duke University Medical Center, Sensory Plasticity Laboratory, Durham, North Carolina 27710

Background: The chemerin-CMKLR1 axis modulates inflammation; ligands for CMKLR1 have short half-lives.
Results: We have utilized a novel technology to develop a long-acting, high potency membrane-anchored CMKLR1 agonist.
Conclusion: This ligand decreases allergic airway inflammation and neuropathic pain in mice.
Significance: Our approach can be applied to develop other candidate therapeutics targeting peptide hormone receptors implicated as modulators of disease.

The chemerin receptor (CMKLR1) is a G protein-coupled receptor found on select immune, epithelial, and dorsal root ganglion/spinal cord neuronal cells. CMKLR1 is primarily coupled to the inhibitory G protein, $G\alpha_i$, and has been shown to modulate the resolution of inflammation and neuropathic pain. CMKLR1 is activated by both lipid and peptide agonists, resolvin E1 and chemerin, respectively. Notably, these ligands have short half-lives. To expedite the development of long acting, stable chemerin analogs as candidate therapeutics, we used membrane-tethered ligand technology. Membrane-tethered ligands are recombinant proteins comprised of an extracellular peptide ligand, a linker sequence, and an anchoring transmembrane domain. Using this technology, we established that a 9-amino acid-tethered chemerin fragment (amino acids 149–157) activates both mouse and human CMKLR1 with efficacy exceeding that of the full-length peptide (amino acids 21–157). To enable *in vivo* delivery of a corresponding soluble membrane anchored ligand, we generated lipidated analogs of the 9-amino acid fragment. Pharmacological assessment revealed high potency and wash resistance (an index of membrane anchoring). When tested *in vivo*, a chemerin SMAL decreased allergic airway inflammation and attenuated neuropathic pain in mice. This compound provides a prototype membrane-anchored peptide for the treatment of inflammatory disease. A parallel approach may be applied to developing therapeutics targeting other peptide hormone G protein-coupled receptors.

The chemerin receptor (CMKLR1 or ChemR23)[2] is a chemokine like G protein-coupled receptor (GPCR) expressed on selected populations of cells including inflammatory mediators (macrophages, monocytes, plasmacytoid/myeloid dendritic cells and natural killer cells), epithelial cells, as well as neurons and glial cells in the dorsal root ganglion, spinal cord, and retina (1–3). CMKLR1 is primarily coupled to the inhibitory G protein, $G\alpha_i$ (4). Activation of CMKLR1 has been shown to be pro-resolving and anti-nociceptive in animal models of asthma and pain, respectively (2, 5). Endogenous ligands for this GPCR include both lipid and peptide agonists, resolvin E1 (RvE1) and chemerin, respectively (4, 6). These natural ligands for CMKLR1 have short half-lives due to rapid inactivation, necessitating the development of long acting, stable agonists.

Chemerin is produced as a 163-amino acid protein (4). Following cleavage of its signal sequence, chemerin(21–163) is secreted as an inactive 143-residue prohormone (7). Proteolytic cleavage of 6 amino acids at the C terminus converts the prohormone into the full-length active peptide (chemerin(21–157)) (8). Biological activity of chemerin is dependent on C-terminal processing. In light of this functional requirement, the focus of our study is on peptides derived from this domain. Short, C-terminal fragments of chemerin have been shown to activate CMKLR1 albeit with less potency than full-length chemerin (chemerin(21–157)) (9). Advantages of smaller peptides include expedited synthesis and a wider range of delivery modes. Remaining challenges in optimizing short peptides for *in* vivo use include increasing potency, efficacy, and stability.

[1] To whom correspondence should be addressed: 800 Washington St., P.O. Box 7703, Boston, MA 02111. Tel.: 617-636-4834; Fax: 617-636-8692; E-mail: akopin@tuftsmedicalcenter.org.

[2] The abbreviations used are: CMKLR1/ChemR23, chemerin receptor; MTL, membrane-tethered ligand; SMAL, soluble membrane-anchored ligand; GPCR, G protein-coupled receptor; OVA, ovalbumin; CCI, chronic constriction injury; Fmoc, *N*-(9-fluorenyl)methoxycarbonyl; BALF, BAL fluid; DMSO, dimethyl sulfoxide; s-Stable Chem, soluble stable chemerin peptide; l-Stable Chem, lipidated stable chemerin peptide.

Development of a Membrane-anchored Chemerin Agonist

We have recently established the utility of membrane tethered ligands (MTLs) as modulators of GPCR signaling both *in vitro* and *in vivo* (10, 11). These recombinant constructs encode a membrane-anchoring sequence and a flexible protein linker that tethers the peptide ligand in the extracellular space. MTLs can be designed so that the construct has either a free amino- or carboxyl-terminal extracellular end depending on the ligand activity determinants (11, 12). Given the importance of the C-terminal end of chemerin, we initiated experiments by incorporating a type II transmembrane domain anchor into the chemerin MTL (13). This transmembrane domain configuration positions the C-terminal end of chemerin into the extracellular space, thus enabling interaction with its cognate GPCR, CMKLR1. MTLs, by virtue of the ease of modifying the corresponding cDNA, offer an expedited approach for generating and assaying variant peptides thus enabling identification of functionally optimized constructs (14).

One limitation of MTLs is that they are recombinant proteins that require expression of the corresponding cDNA. To enable direct administration of anchored peptides *in vivo*, we converted an optimized MTL into a lipidated peptide, thus generating a soluble membrane-anchored ligand (SMAL). The SMAL was designed with a putative membrane anchor, a lipid-PEG linker, covalently attached to the peptide ligand, with the objective of creating a synthetic mimic of the MTL. As anticipated, our efforts ultimately resulted in a long acting, high potency, wash-resistant CMKLR1 agonist. When assessed *in vivo*, this molecule decreased allergic airway inflammation and attenuated neuropathic pain, highlighting the therapeutic potential of this novel lipidated compound.

EXPERIMENTAL PROCEDURES

Recombinant GPCR and Tethered Ligand Constructs—Plasmids encoding either the human (University of Missouri cDNA Resource Center) or the mouse (Origene) chemerin receptor cDNA were purchased and subcloned into pcDNA1.1. The full-length human chemerin cDNA (encoding pre-prochemerin corresponding to amino acids 1–163) was purchased from Sino Biological. The chemerin coding region was PCR amplified and subcloned into a type II MTL backbone as previously described (12). The corresponding MTL cDNA encodes a TNFα transmembrane domain, a "GN" repeat linker containing a c-Myc tag (to monitor MTL expression levels), and the chemerin peptide at the C terminus. The TNFα transmembrane domain, by virtue of it being a type II transmembrane domain, positions the MTL such that the C terminus of the construct projects into the extracellular space (13). This orientation is optimal for the study of chemerin because the C-terminal end of the peptide has been shown to be important for activity at CMKLR1 (9). MTLs encoding pre-prochemerin (amino acids 1–163), full-length chemerin (amino acids 21–157), and various C-terminal fragments of chemerin (*i.e.* amino acids 145–157, 149–157, and 141–155) (9, 15) were generated in addition to a negative control MTL (including the amino acid sequence of human galanin). To assess variant chemerin sequences, degenerate oligonucleotides ("NNKNNK" where N = A, C, G, or T and K = G or T) were used to introduce variability at positions corresponding to the 2 carboxyl-terminal residues of chemerin(149–157)

(amino acids 156 and 157). The nucleotide sequences of all receptor and tether constructs were confirmed using automated DNA sequencing followed by analysis with VectorNTI (Invitrogen).

Synthesis of Lipidated Peptides—All commercial reagents were used without further purification. *N*-tert-Butoxycarbonyl (*N*-Boc) protected D- and L-amino acids and 4-hydroxymethyl-phenylacetamidomethyl resin modified with *N*-Boc-L-Ser were purchased from Chemimpex. 2-(1*H*-Benzotriazol-1-yl)-1,1,3,3-tetramethyluronium hexafluorophosphate was procured from Novabiochem. Monodisperse, hetero-bifunctional polyethylene glycol (PEG), *N*-Fmoc-PEG8-propionic acid, and the unnatural amino acid Boc-(3S)-1,2,3,4-tetrahydroisoquinoline-3-carboxylic acid (*N*-Boc-L-Tic-OH) were from AAPPTec. Palmitic acid was purchased from Sigma. Hydrogen fluoride was from Matheson Tri-Gas. Solvents for reversed-phase high performance liquid chromatography (RP-HPLC) had the following composition: solvent A, $H_2O/CH_3CN/$trifluoroacetic acid (TFA) (99/1/0.1); solvent B, $CH_3CN/H_2O/$TFA (90/10/0.07).

Peptides were manually assembled using the *in situ* neutralization protocol for *t*-Boc chemistry (16) on 4-hydroxymethyl-phenylacetamidomethyl resin on a 0.5-mmol scale. Amino acids, both L and D were used with the following side chain protecting groups: Gln(Xan), Lys (Fmoc), Ser(Bzl), and Tyr(2-Br-Z). Peptide coupling reactions were carried out with a 4-fold excess (2.0 mmol) of activated amino acid for at least 15 min. The *t*-Boc protecting group on the N terminus was removed using TFA. Both resins were split into two equal portions. One portion was used for synthesizing the non-lipidated peptides. The chemerin 9 peptide (s-Chem(149–157)) on resin was acetylated at the N terminus before cleavage; the stable chemerin peptide (s-Stable Chem) was left unmodified at the N terminus. These peptides served as positive controls for the lipidated peptides. The free N terminus was first pegylated with *N*-Fmoc-PEG8-propionic acid using standard 2-(1*H*-benzotriazol-1-yl)-1,1,3,3-tetramethyluronium hexafluorophosphate coupling conditions. The *N*-Fmoc protecting group was removed by treatment with 10% piperidine in *N,N*-dimethylformamide for 5 min. Palmitic acid was subsequently coupled with the N-terminal free amine of the pegylated peptide. Peptides were cleaved from the resin by using high hydrofluoric acid conditions (17) (90% anhydrous hydrofluoric acid, 10% anisole at 0 °C for 1.5 h) and precipitated with cold Et_2O. Unmodified peptides were extracted using 10% AcOH in water and the lipidated peptides were extracted using 10% AcOH in water followed by 10% AcOH in 50% $EtOH/H_2O$. Crude peptides were purified by RP-HPLC (Vydac C18, 10 μm, 22 × 250 mm). The purities of the peptides were assessed by analytical RP-HPLC (Vydac C18, 5 μm, 4 × 250 mm). The molar mass of peptides was determined by MALDI-TOF MS. Peptide concentrations were determined using tyrosine absorbance ($\epsilon = 1400$ M^{-1} cm^{-1} at 278 nm) (18). The soluble control peptide for chemerin 9 (s-Chem(149–157)) included a KGG spacer coupled to the N terminus to allow attachment of the corresponding PEG8-palmitic acid and provide a handle for further modification with fluorophores. In comparison, the soluble stable chemerin analog (s-Stable Chem) did not contain the GG spacer used for subsequent anchoring. Detailed information on

TABLE 1
Chemical structure, purity, and molecular weight of synthesized peptides

s-Chem 149-157

l-Chem 149-157

s-Stable Chem

H₂N-Y*-F-L-P S*-Q-F A*-Tic-S-COOH

l-Stable Chem

Y*, S* and A* are D - amino acids

Tic

Peptides	HPLC Purity[a] (%)	Molecular Weights (Da)	
		Calculated[b]	Observed[c]
s-Chem 149-157[d]	97	1388.64	1411.7 [M+Na]+
l-Chem 149-157[d]	98	2009.11	2007.8 [M-H]-
s-Stable Chem	99	1217.58	1218.5 [M+H]+
l-Stable Chem[e]	98	1994.10	1993.4 [M-H]-

[a] Purity was determined by analytical RP-HPLC (Vydac C18, 5 μm, 4 × 250 mm) and a binary solvent system (A: H_2O/CH₃CN/TFA (99/1/0.1); B: CH₃CN/H_2O/TFA (90/10/0.07)) with a linear gradient of solvent B over 20 min. Flow rate was at 1 ml/min and elution was monitored at by absorbance at 230 nm.

[b] Expected molecular weights were calculated using Peptide mass calculator version 3.2.

[c] Observed molecular weights were determined by MALDI-TOF MS in positive reflectron mode using α-cyano-4-hydroxycinnamic acid as the matrix.

[d] KGG spacer coupled to the N terminus of the peptide before pegylation.

[e] GG spacer coupled to the N terminus of the peptide before pegylation.

chemical structures, purities, and molecular weights of the synthetic peptides are listed in Table 1.

Cell Culture—Human embryonic kidney (HEK) 293 cells were cultured in Dulbecco's modified Eagle's medium (Invitrogen) with 10% fetal bovine serum (Atlanta Biologicals), 100 units/ml of penicillin, and 100 μg/ml of streptomycin. Cells were maintained at 37 °C in a humidified environment with 5% CO_2.

Luciferase Reporter Gene Assays—Receptor-mediated signaling was assessed as previously described (19). Briefly, HEK293 cells were plated at a density of 6,000 cells/well into 96-well clear-bottom plates and grown to ~80% confluence. Cells were transiently transfected with PEI (0.1 μl/well of a 1 mg/ml of solution) in serum-free media (20) with cDNAs encoding (*a*) human or mouse chemerin receptor (or pcDNA1.1 as an empty expression vector), (*b*) a tethered ligand (where applicable), (*c*) an SRE-luciferase reporter gene with a PEST degradation sequence (SRE$_{5x}$-Luc-PEST), (*d*) G$_{q5i66V}$, a chimeric Gα$_q$ protein containing the five carboxyl-terminal amino acids corresponding to Gα$_i$ and valine substitution at amino acid position 66, and (*e*) β-galactosidase (control for transfection efficiency). Expression of G$_{q5i66V}$ directs signaling of the Gα$_i$-coupled chemerin receptor to stimulation of a Gα$_q$-dependent SRE$_{5x}$-Luc-PEST reporter gene (21, 22). For experiments investigating the agonist function of soluble and lipidated peptides, tethered ligand cDNA was not included in the transfection mixture.

Twenty-four hours after transfection, cells were stimulated with or without peptide agonist for 4 h in serum-free medium. Recombinant human chemerin (corresponding to amino acids 21–157) was purchased from R & D Systems, and chemerin(145–157) was purchased from Phoenix Pharmaceuticals. Lipidated peptides and corresponding soluble ligands were synthesized as described above. Following ligand stimulation, the media was aspirated, and luciferase activity was measured using SteadyLite reagent and quantified using a Top-Count NTX. A β-galactosidase assay was then performed following assessment of luminescence. Cleavage of 2-nitrophenyl β-D-galactopyranoside substrate was quantified after incubation of cell lysates at 37 °C for 30 to 60 min by measuring the optical density at 420 nm on a SpectraMax microplate reader. Luciferase reporter gene activities were normalized to corresponding β-galactosidase activity controls.

Washout Experiments—Agonist activity was compared with and without serial washings shortly after addition of ligand as previously described (14, 23). Briefly, HEK293 cells were plated and transfected as described above with the addition of a poly-L-lysine plate pretreatment step to enhance cell adhesion. Twenty-four hours after transfection, cells were stimulated with increasing concentrations of agonist for 15 min at 37 °C. Selected wells were washed three times with serum-free medium. Plates were then incubated for an additional 4 h. Receptor-mediated signaling was assessed using a luciferase-based assay as described above.

Ovalbumin Sensitization and in Vivo Chemerin Administration—Male FVB mice age 5–7 weeks (Charles River Laboratories) were housed under viral antibody-free conditions. OVA sensitization and drug administration were performed as previously described with slight modifications (5). Briefly, mice were sensitized by intraperitoneal injection of 10 μg of OVA (Grade III: Sigma) plus 1 mg of aluminum hydroxide as adjuvant (Sigma) in 0.2 ml of saline on days 0 and 7. On days 14, 15, 16, and 17, mice received a 25-min aerosol challenge of 6% (w/v) OVA each day. On each of these days, 30 min prior to OVA challenge, mice were given 20 μl of s-Chem(149–157), s-Stable chemerin, or l-Stable chemerin (21 mM stock in DMSO diluted 1:100 in saline for a final concentration of 210 μM) by the intranasal route. Corresponding vehicle controls received DMSO diluted 1:100 in saline. On day 18, lungs were fixed in 10% (v/v) formalin and embedded in paraffin for staining with periodic acid-Schiff reagent (Sigma).

In another series of experiments, mice were treated with l-Stable Chem or DMSO control as described above. On day 18, lungs were fixed and stained with hematoxylin and eosin (H&E, Sigma). In a separate cohort of mice, bronchoalveolar lavage (24) was performed with two 1-ml aliquots of PBS with 0.6 mM EDTA. Cells in BAL fluids (BALFs) were resuspended in PBS and counted using a hemocytometer. Cytospin preparations were done by cytocentrifugation (265 × *g*; StatSpin), and cells were stained with Wright-Giemsa stain (Sigma) for quantification of leukocyte subsets. At least 200 cells were counted per slide.

For non-OVA control experiments, mice received l-Stable Chem (21 mM stock in DMSO diluted 1:100 in saline for a final concentration of 210 μM) or DMSO for 4 consecutive days (cor-

responding to days 14, 15, 16, and 17 of the OVA studies). On the 5th day (corresponding to day 18) mice were sacrificed, and BALF was collected and analyzed as described above.

Neuropathic Pain Model and Behavioral Analysis—Adult CD1 mice (male, 25–35 g) were used for the behavioral studies. Mice were group-housed and kept under a 12-h light/dark cycle. For the neuropathic pain model, chronic construction injury (25) was induced by ligation of the sciatic nerve under isoflurane anesthesia (26, 27). For intrathecal injection, spinal cord puncture was made with a 30-guage needle between the L5 and L6 level to deliver reagents (10 μl) to the cerebral spinal fluid. l-Stable Chem was synthesized as described above. RvE1 was kindly provided by Resolvyx Pharmaceuticals Inc. as a gift to Ru-Rong Ji.

Nerve injury-induced mechanical allodynia and hypersensitivity were assessed by von Frey hairs as previously described (28). For testing mechanical sensitivity, the plantar surface of a hindpaw was stimulated with a series of von Frey hairs (0.02–2.56 g, Stoelting). The 50% paw withdrawal threshold was determined using Dixon's up-down method. For paw withdrawal frequency, the same von Frey hair (0.16 g) was applied 10 times and the number of positive responses to the stimulations counted. A positive response was scored if the mouse sharply withdrew the paw or flinched upon removal of the stimulus. Cold allodynia was tested by the acetone method as previously reported (29). In brief, a drop of acetone was placed against the plantar paw of the mouse and the response of the mouse monitored for the next 20 s. If there was no response then a score of 0 was assigned. If there was a response, this response was monitored 40 s in total and behavior was assigned as follows: 1, quick withdrawal or stamp of the foot; 2, prolonged withdrawal and repeated flicking of the paw; 3, repeated flicking of the paw with licking directed at the ventral side of the paw.

Data Analysis—EC_{50} values were determined by nonlinear curve fitting using GraphPad Prism 6.0 software. Statistical comparisons were made using either t test or one-way analysis of variance with Tukey's post hoc test. Data were considered to be statistically significant with $p < 0.05$.

RESULTS

Soluble Full-length and C-terminal Human Chemerin Peptides Activate Human and Mouse CMKLR1—In this study, we first compared the activation of human and mouse CMKLR1 with commercially available peptides using a luciferase reporter assay. Full-length chemerin (s-Chem(21–157)) activates human CMKLR1 with higher potency than the C-terminal 13-amino acid fragment (s-Chem(145–157)) (Fig. 1a). These two human peptides also activate mouse CMKLR1, again with s-Chem(21–157) potency exceeding that of s-Chem(145–157) (Fig. 1b). The EC_{50} values for these peptides (Table 2) are best approximations given that a supramaximal ligand concentration was not included. Even with this limitation, the shift in the concentration-response curves reflects a potency difference between the ligands.

Tethered Full-length and C-terminal Human Chemerin Peptides Activate Both Human and Mouse Receptors—As a next step, we examined how membrane anchoring would influence chemerin activity. To pursue these studies, we made MTL con-
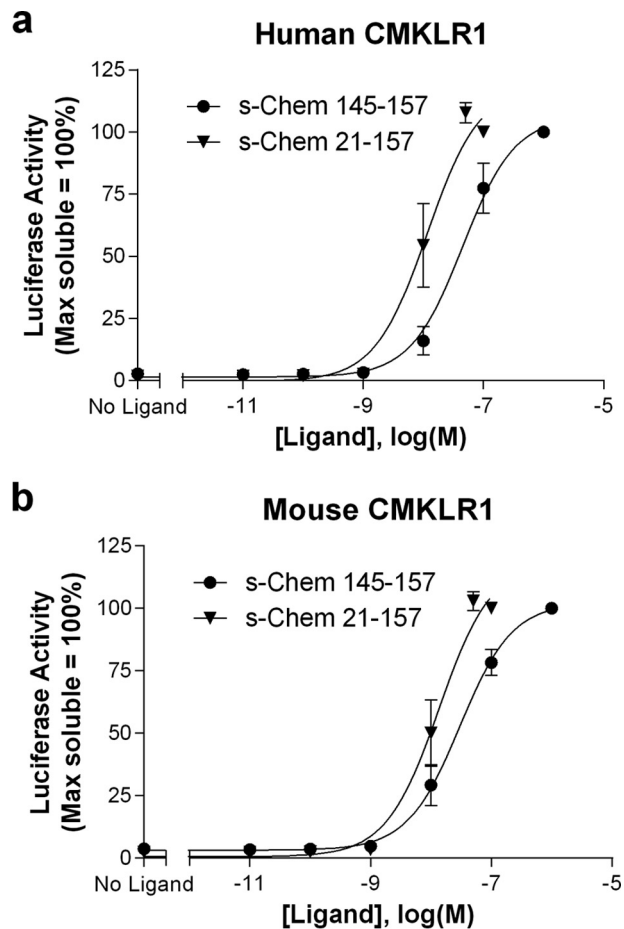

FIGURE 1. **Soluble full-length chemerin (s-Chem(21–157)) has higher potency than soluble chemerin(145–157) at both human (*a*) and mouse (*b*) CMKLR1.** s-Chem(145–157) and s-Chem(21–157) were purchased commercially. HEK293 cells were transiently transfected with cDNAs encoding (i) human or mouse CMKLR1, (ii) a SRE$_{5x}$-Luc-PEST reporter gene, (iii) a Gα_{q5i66V} chimera, and (iv) a β-galactosidase control. Twenty-four hours after transfection cells were stimulated with ligand for 4 h and luciferase activity was determined as described under "Experimental Procedures." Luciferase activity was normalized relative to the maximal value observed using saturating concentrations of the corresponding soluble ligand (=100%). Data points represent the mean $\pm$ S.E. from at least three independent experiments, each performed in triplicate.

structs encoding various length chemerin fragments (as described under "Experimental Procedures") and assessed activity at both the human and mouse receptors. Representative tethers are illustrated in Fig. 2. Surprisingly, the shortest tether tested (t-Chem(149–157) corresponding to the C-terminal 9 amino acids of chemerin) had the highest activity on the human receptor (Fig. 2a), even when compared with the full-length peptide (t-Chem(21–157)). In contrast, preprochemerin (t-Chem(1–163)) did not activate either receptor consistent with a requirement for C-terminal processing for chemerin signaling (8). In addition, a negative control tether encoding the sequence for human galanin did not activate either receptor. Additional controls were performed to determine whether the increased activity of t-Chem(149–157) could be explained by differential expression of tethered constructs. Expression of both tethered constructs were assessed using an ELISA. The enhanced activity of t-Chem(149–157) was not an artifact of increased expression of t-Chem(149–157) (*versus* t-Chem(21–157); data not shown).

TABLE 2

Half-maximal effective concentration (EC_{50}) for each CMKLR1 ligand with corresponding pEC_{50}

All values represent the mean ± S.E. from at least three independent experiments, each performed in triplicate. s-Chem(145–157) and s-Chem(21–157) were purchased commercially. All other structures are shown in Table 1. Abbreviations: s-Chem(21–157) (soluble recombinant human chemerin corresponding to amino acids 21–157), s-Chem(149–157) (soluble C-terminal 9 amino acids of human chemerin), l-Chem(149–157) (lipidated C-terminal 9 amino acids of human chemerin), s-Stable Chem (soluble stable chemerin peptide), l-Stable Chem (lipidated stable chemerin peptide).

Ligand	Wash	Human CMKLR1		Mouse CMKLR1	
		EC_{50}	pEC_{50}	EC_{50}	pEC_{50}
		nM		nM	
s-Chem(145–157)	−	45.1	7.37 ± 0.16	30.1	7.52 ± 0.17
s-Chem(21–157)	−	11.7	8.02 ± 0.19	13.7	8.01 ± 0.20
s-Chem(149–157)	−	139.3	6.85 ± 0.08	59.3	7.22 ± 0.07
l-Chem-(149–157)	−	4.3	8.35 ± 0.10	4.0	8.38 ± 0.10
s-Chem(149–157)	+	‡‡[a]	‡‡	‡‡	‡‡
l-Chem(149–157)	+	90.2	7.07 ± 0.13	42.9	7.39 ± 0.09
s-Stable Chem	−	60.6	7.21 ± 0.08	11.9	7.92 ± 0.06
l-Stable Chem	−	2.6	8.59 ± 0.09	2.0	8.70 ± 0.09
s-Stable Chem	+	‡‡	‡‡	‡‡	‡‡
l-Stable Chem	+	27.1	7.60 ± 0.18	10.4	7.96 ± 0.16

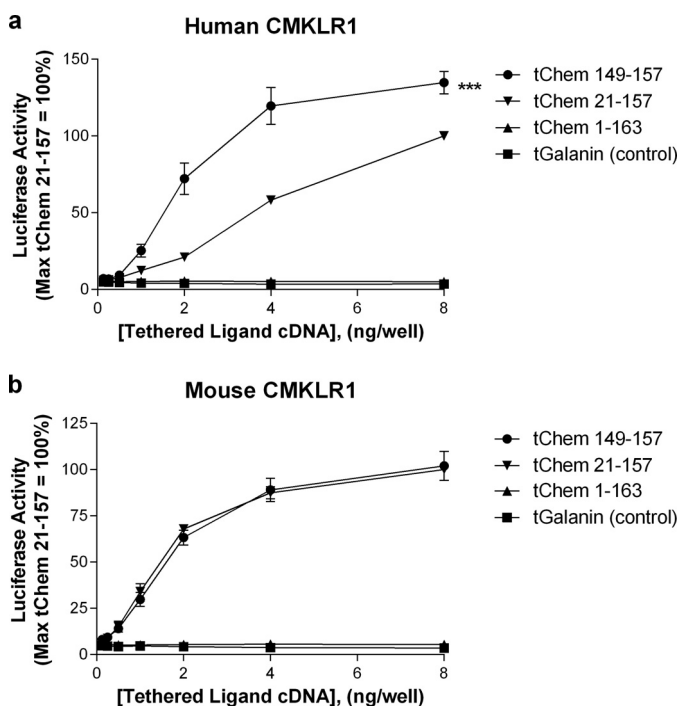[a] ‡‡, insufficient signal to calculate EC_{50}.

FIGURE 2. Tethered chemerin 9 (t-Chem(149–157)) activity exceeds that of full-length chemerin (t-Chem(21–157)) at the human receptor (*a*). In contrast, activation of the mouse receptor by these two constructs is comparable (*b*). Pre-prochemerin (t-Chem(1–163)) and the control (tGalanin) lack activity at both human and mouse receptors. HEK293 cells were transiently transfected with cDNAs encoding (i) indicated tethered ligand, (ii) human or mouse CMKLR1, (iii) a SRE$_{5x}$-Luc-PEST reporter gene, (iv) a Gα$_{q5i66v}$ chimera, and (v) a β-galactosidase control. Twenty-four hours after transfection, luciferase activity was determined as described under "Experimental Procedures." Luciferase activity was normalized relative to the maximal value observed using t-Chem(21–157) cDNA (=100%). Data points represent the mean ± S.E. from at least three independent experiments, each performed in triplicate. Comparison of t-Chem(21–157) to t-Chem(149–157) is shown: ***, $p < 0.001$.

The MTL Platform Can Be Used to Generate a Series of Chemerin Ligands with Varying Activities—In light of the enhanced activity of t-Chem(149–157) at the human receptor, we next explored whether modification of the endogenous chemerin sequence could further potentiate ligand-mediated signaling. To assess this possibility, we screened ~200 constructs encoding t-Chem(149–157) with variability at positions 156 and 157. Amino acids 156 and 157 were chosen because they are established CMKLR1 activity determinants (9).

Selected results of the screen are highlighted in Fig. 3. As shown in Fig. 3*a*, the endogenous sequence ("FS") had comparable activity to "VA" at human CMKLR1 with "SL" showing partial agonist activity, and "GP"/"GH" illustrating no activity. In comparison, FS and VA both activated mouse CMKLR1 with both SL/GP showing partial agonist activity and GH showing no effect. Again, negative control tethered galanin did not activate either receptor. Because the endogenous Chem(149–157) sequence showed the highest activity as a tether, we chose to utilize this sequence in follow-up experiments.

Lipidation of Chem(149–157) Confers Enhanced Potency and Wash-resistant Activity—Based on our results with tethered *versus* soluble chemerin(149–157), we hypothesized that the enhanced activity on human CMKLR1 was due to membrane anchoring. We thus postulated that a SMAL would also show increased activity and have the additional advantage that it could be directly delivered for *in vivo* testing. We therefore synthesized a lipidated counterpart of Chem(149–157) (Table 1), a putative CMKLR1 SMAL. Lipidation of the C-terminal 9 amino acids of chemerin (l-Chem(149–157)) enhanced potency of the ligand at both the human and mouse CMKLR1 when compared with the soluble peptide (s-Chem(149–157)) (Fig. 4, *a* and *c*; Table 2). To determine whether the lipidated peptide was anchored in the cell membrane, we performed washout experiments on both human and mouse CMKLR1 receptors. Despite serial washes after the addition of ligand, the activity of l-Chem(149–157) persisted, whereas only trace agonist-induced signaling was observed with the soluble ligand (Fig. 4, *b* and *d*; Table 2). Signaling by both s-Chem(149–157) and l-Chem(149–157) required expression of CMKLR1; no agonist activity was observed when cells were transfected with vector control (*i.e.* pcDNA1.1; data not shown).

A Lipidated, Stable Chemerin Analog Activates Human and Mouse CMKLR1 with High Potency and Wash Resistance—It has been previously shown that chemerin is rapidly inactivated *in vivo* by proteases. To further enhance the activity and half-life of the lipidated chemerin analog, a proteolysis resistant chemerin sequence (30) was introduced into our construct (Table 1). Lipidation of this peptide led to enhanced potency at both human and mouse receptors (Fig. 5, *a* and *c*; Table 2). Furthermore, the activity of the lipidated stable peptide per-
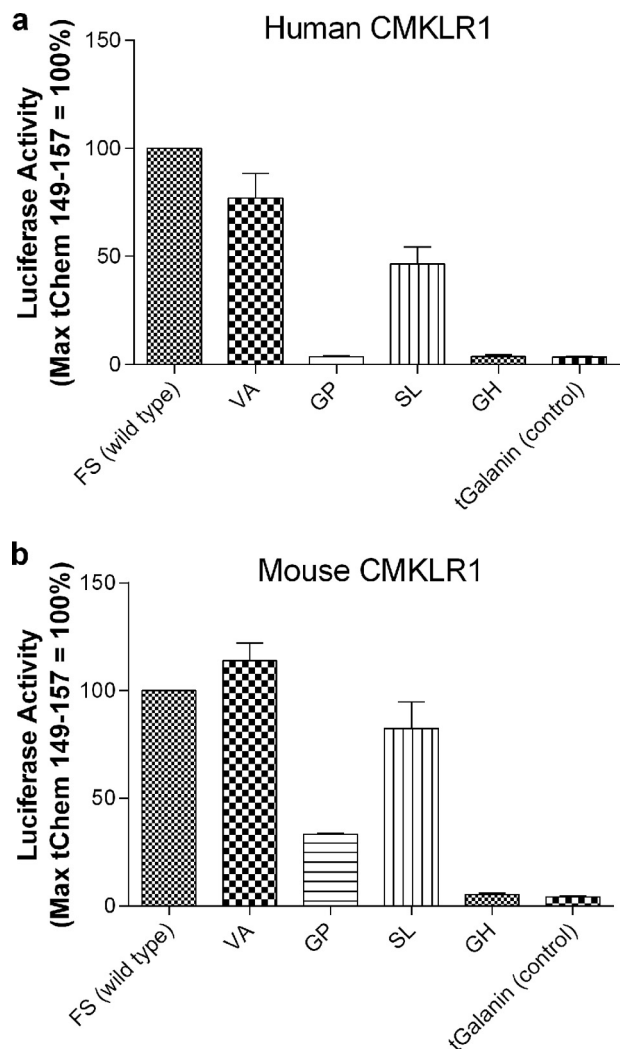
a

Human CMKLR1

b

Mouse CMKLR1

FIGURE 3. **Modifying the two C-terminal amino acids of t-Chem(149–157) results in MTLs with varying degrees of activity on human (*a*) and mouse (*b*) CMKLR1.** HEK293 cells were transiently transfected with cDNAs encoding (i) 8 ng of the indicated tethered ligand, (ii) human or mouse CMKLR1, (iii) a SRE$_{5x}$-Luc-PEST reporter gene, (iv) a Gα_{q5i66v} chimera, and (v) a β-galactosidase control. Twenty-four hours after transfection, luciferase activity was determined as described under "Experimental Procedures." Luciferase activity was normalized relative to the maximal value observed with t-Chem(149–157) cDNA (=100%). Data points represent the mean ± S.E. from at least three independent experiments, each performed in triplicate.

sisted despite washing, whereas the activity of the soluble counterpart rapidly decreased when assessed at both the human and mouse receptors (Fig. 5, *b* and *d*; Table 2). Signaling by both s-Stable Chem and l-Stable Chem required expression of CMKLR1; no agonist activity was observed when cells were transfected with vector control (*i.e.* pcDNA1.1; data not shown).

l-Stable Chemerin Exhibits in Vivo Activity and Abrogates Allergic Airway Responses in Mice—CMKLR1 was previously suggested to modulate lung inflammation in an LPS model (31). Based on this prior report, we wanted to further explore and extend the role of this receptor in allergic airway responses. Given the high potency, stability, and wash resistance of the lipidated stable chemerin analog, we postulated that it may modulate airway remodeling and the inflammatory response known to occur in our *in vivo* model. To test this hypothesis, we

used an allergen sensitization and airway challenge model where mice were first sensitized with OVA followed by OVA aerosol challenge. In this model, s-Chem(149–157), s-Stable Chem, or l-Stable Chem were administered prior to each OVA aerosol challenge (Fig. 6*A*). As illustrated in Fig. 6*B*, significant changes in airway epithelial mucus (*versus* DMSO control) were apparent in all treatment groups as determined by periodic acid-Schiff reagent staining at low magnification (×20). The most pronounced attenuation of mucus metaplasia was seen in mice treated with l-Stable Chem.

To further probe the effects of l-Stable Chem, we also examined the inflammatory response in the lung using H&E staining and BALF analysis of leukocytes. Following visual assessment of histological sections taken from mice treated with l-Stable Chem, we observed less leukocyte infiltration and fewer reactive bronchial epithelial cells in comparison to DMSO control (Fig. 6*C*). Accompanying cell counts confirmed an anti-inflammatory effect of treatment with l-Stable Chem. In BALF taken from DMSO *versus* l-Stable Chem-treated mice, leukocyte infiltrates were quantified and showed a significant reduction in the number of eosinophils at day 18 (Fig. 6*D*).

To test if there were any changes induced by l-Stable Chem alone, a subset of non-OVA sensitized mice was assessed. Here, mice were administered l-Stable Chem or DMSO control for 4 days and sacrificed on the 5th day. No evident inflammation in either cohort was observed. BALF from these cohorts revealed no differences in leukocyte numbers between groups with only resident macrophages present (data not shown). In each of the above experiments, mice in all 4 treatment groups (DMSO, s-Chem(149–157), s-Stable Chem, l-Stable Chem) appeared healthy throughout the protocol.

l-Stable Chemerin Decreases Mechanical and Cold Hypersensitivity in an Experimental Model of Neuropathic Pain: Comparison to Resolvin E1 (RvE1)—We examined whether treatment with l-Stable Chem would reduce nerve injury-induced neuropathic pain. We compared these results to RvE1 to determine whether l-Stable Chem would provide a more protracted attenuation of pain responses. Chronic construction injury (25) of the sciatic nerve produced robust mechanical allodynia as indicated by a reduction in paw withdrawal threshold in response to a series of von Frey hairs (Fig. 7, *A* and *B*) and an increase in paw withdrawal frequency in response to a specific low-threshold von Frey hair (0.16 g, Fig. 7, *C* and *D*). CCI-induced neuropathic pain is also characterized by cold allodynia, a nociceptive response to acetone stimulation (Fig. 7, *E* and *F*). These are cardinal features of neuropathic pain, elicited by normally innocuous stimuli. Notably, treatment with l-Stable Chem via spinal intrathecal route (100 pmol), 1 week following nerve injury when neuropathic pain is fully developed, significantly reduced established mechanical and cold allodynia for greater than 24 h (Fig. 7, *A*, *C*, and *E*). In comparison, the effects of RvE1 were only transient, with a significant decrease in pain scores observed only at the 1-h time point (Fig. 7, *B*, *D*, and *F*).

DISCUSSION

In the current study, we explored the effects of recombinant and synthetic membrane anchoring on the activity of
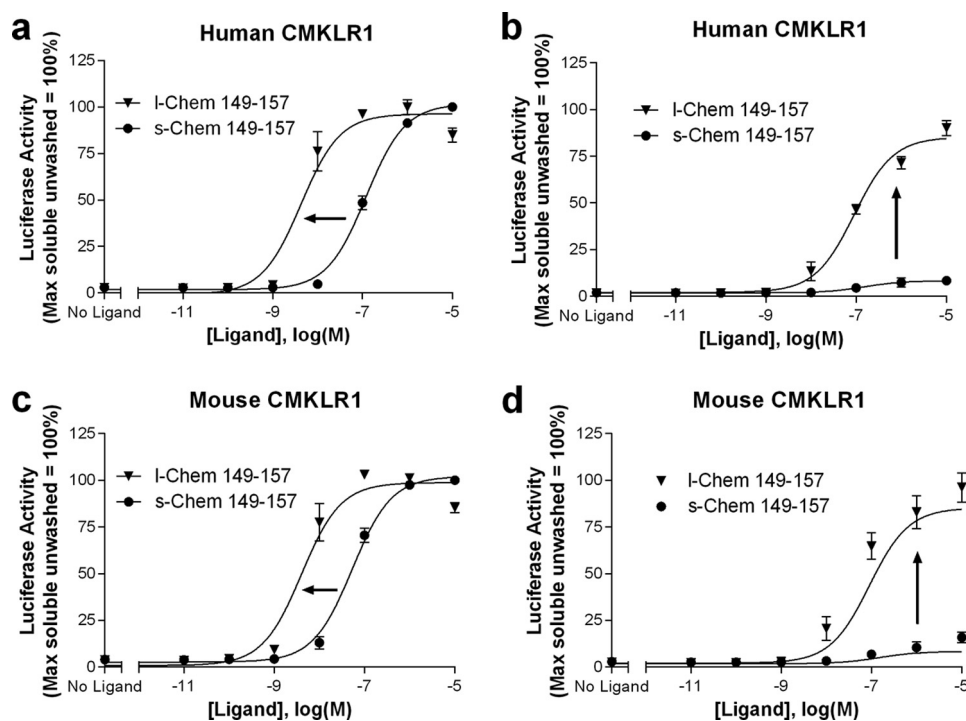
FIGURE 4. **Lipidation of chemerin(149–157) (l-Chem(149–157)) enhances potency at both the human (*a*) and mouse (*c*) receptors.** Activity of this analog remains following serial washes *versus* activity of the soluble peptide (s-Chem(149–157)) at both the human (*b*) and mouse (*d*) receptors. Structures of s-Chem(149–157) and l-Chem(149–157) are shown in Table 1. HEK293 cells were transiently transfected with cDNAs encoding: (i) human or mouse CMKLR1, (ii) a SRE_{5x}-Luc-PEST reporter gene, (iii) a $G\alpha_{q5i66v}$ chimera, and (iv) a β-galactosidase control. Twenty-four hours after transfection, cells were stimulated with increasing concentrations of the indicated ligands for 15 min. Selected wells were then washed three times with serum-free media and plates were further incubated for 4 h. Luciferase activity, determined as described under "Experimental Procedures," was normalized relative to the maximal value observed using saturating concentrations of s-Chem(149–157) in cells that were unwashed (=100%). Data points represent the mean ± S.E. from at least three independent experiments, each performed in triplicate.

chemerin-derived compounds as well as their impact on inflammation and neuropathic pain. Our analysis included defining ligand efficacy on mouse CMKLR1 in anticipation of preclinical studies, as well as on the human receptor in light of our long term goal of developing therapeutics. We ultimately identified a lipidated chemerin analog, a SMAL, which activates both CMKLR1 species orthologs with high potency. Our studies demonstrated that this stable chemerin receptor agonist has potent *in vivo* efficacy in mouse models of allergic airway inflammation and neuropathic pain.

As an initial step, we established an assay for assessing CMKLR1 signaling induced by chemerin peptides. Comparison of full-length soluble human chemerin (s-Chem(21–157)) at both the mouse and human receptors revealed similar potencies. The high potency of human s-Chem(21–157) on the mouse receptor could not have been fully anticipated given that the sequence identity between these full-length orthologs is only 63% (8). Notably, the mouse and human receptors are 88% homologous. Together these results support the premise that modified CMKLR1 ligands can be developed that target the human receptor yet are amenable to testing using *in vivo* mouse models (*i.e.* agonists show similar potency on both receptors). This is further supported by the occurrence of six identical amino acids at the C terminus of mouse and human chemerin, a domain that is critical for efficacy.

To begin our investigation of the pharmacological properties of membrane-anchored chemerin, we generated recombinant MTLs incorporating selected human chemerin fragments into

the construct. Previous reports in the literature highlighted the C-terminal end of chemerin as the critical activity determinant (9). Therefore, we chose to use a type II MTL that enabled the C-terminal end to freely extend into the extracellular space and activate the receptor (12, 13). Comparison of the full-length (Chem(21–157)) and short chemerin fragments as soluble ligands revealed that Chem(21–157) was the most potent peptide. In contrast, as a tethered ligand, t-Chem(149–157) was more active than the corresponding full-length peptide. The enhanced activity of the 9 C-terminal amino acids of chemerin was unique to the human receptor; activities of both tethered peptides were comparable at the mouse receptor. The importance of C-terminal processing of chemerin from the pre-pro-hormone (Chem(1–163)) into the active form (Chem(21–157)) was illustrated as the tethered pre-prohormone did not activate the human or mouse receptor. These data support that Chem(1–163) when recombinantly expressed in HEK293 cells is not processed into the active form (*i.e.* Chem(21–157)). These data highlight the utility of MTLs as tools to investigate inactive *versus* active isoforms of a peptide in addition to discerning the domains (*e.g.* C terminus) that mediate activity of a peptide at its cognate GPCR.

Our investigations also illustrate the utility of MTLs as tools to efficiently generate and characterize functionally altered peptide ligands. In light of the observed increase in signaling of the 9 C-terminal amino acids of chemerin (relative to Chem(21–157)) at the human receptor, we explored whether amino acid substitutions within tethered Chem(149–157)
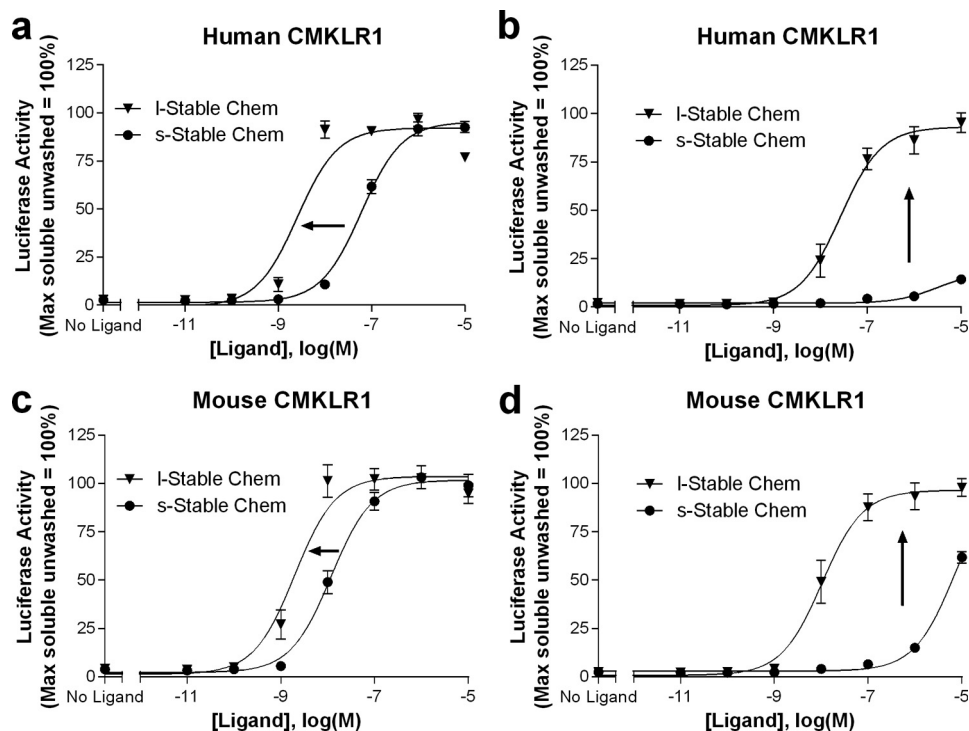
FIGURE 5. **A lipidated, stable chemerin analog (s-Stable Chem) has higher potency than the corresponding soluble peptide.** Activities were compared at both the human (*a*) and mouse (*c*) receptors. Signaling of this analog persists despite serial washes, whereas activity of the soluble counterpart (s-Stable Chem) is markedly diminished at both the human (*b*) and mouse (*d*) receptors. Structures of s-Stable Chem and l-Stable Chem are shown in Table 1. HEK293 cells were transiently transfected with cDNAs encoding: (i) human or mouse CMKLR1, (ii) a SRE$_{5x}$-Luc-PEST reporter gene, (iii) a Gα_{q5i66V} chimera, and (iv) a β-galactosidase control. Twenty-four hours after transfection, cells were stimulated with increasing concentrations of the indicated ligands for 15 min. Selected wells were then washed three times with serum-free media and plates were further incubated for 4 h. Luciferase activity, determined as described under "Experimental Procedures," was normalized relative to the maximal value observed using saturating concentrations of s-Stable Chem in cells that were unwashed (=100%). Data points represent the mean ± S.E. from at least three independent experiments, each performed in triplicate.

would further enhance activity. To this end, we screened a variety of peptide sequences that were modified at amino acid positions 156 and 157. These residues were selected because of their known functional importance in chemerin-mediated activation of CMKLR1 (9). Modification with certain amino acids (*i.e.* position 157: Ser to Ala or Leu) resulted in partial agonists, whereas substitution with other amino acids (*i.e.* position 157: Ser to Pro or His) abolished ligand induced signaling. Assessment of the variant Chem(149–157) MTLs on the human *versus* the mouse receptors reveals similar functional profiles with the exception of the GP analog. This MTL illustrates the potential of even minor alterations in a ligand to result in marked activity differences even when compared at conserved GPCR orthologs.

In this study, in addition to examining effects of recombinant membrane tethering, we generated and pharmacologically characterized peptides with a synthetic lipid membrane anchor. Being aware of the difficulties inherent in delivering recombinant constructs as therapeutics, it was important to explore alternative forms of membrane tethering that would enable delivery of an anchored therapeutic. In light of the enhanced activity of tethered Chem(149–157) at the human receptor (relative to Chem(21–157)), this peptide fragment was selected for further study as a lipidated construct. We utilized synthetic chemistry to generate a 9-amino acid peptide (human Chem(149–157)) linked to palmitic acid via a PEG$_8$ linker (*i.e.* l-Chem(149–157)). The corresponding membrane-anchored

ligand showed enhanced potency and wash resistance in comparison to its soluble counterpart. As illustrated by Chem(149–157), lipidation offers a potential means to enhance potency and/or prolong activity of the ligand via anchoring of the compound into the membrane. Lipidation has been used as a tool to counteract some of the limitations associated with peptide therapeutics (*e.g.* rapid degradation and clearance) and has been successful in optimizing drug leads into therapeutically viable candidates (32).

In addition to lipidation, modification of the peptide sequence to confer protease resistance offers a complementary approach to augmenting agonist function *in vivo*. Many approaches have been taken to decrease the proteolysis of peptides, including, *N*-methylation, ester linkages (α-hydroxy acids), insertion of additional methylene groups into the backbone (β-amino acids, γ-amino acids, etc.), and the use of D-amino acids (33). In particular, enhanced peptide stability by addition of D-amino acids has been demonstrated for a number of peptides that are important mediators of immune-based disorders (34) and neuropathic pain (35). Our strategy was to combine lipidation with alteration of targeted amino acids to confer protease resistance. This strategy offers a platform for generating compounds that are long acting and stable *in vivo*. We illustrate this paradigm by incorporating a protease-resistant peptide sequence (30) in place of Chem(149–157) within the lipidated ligand. This lipidated stable chemerin analog (l-Stable Chem) showed
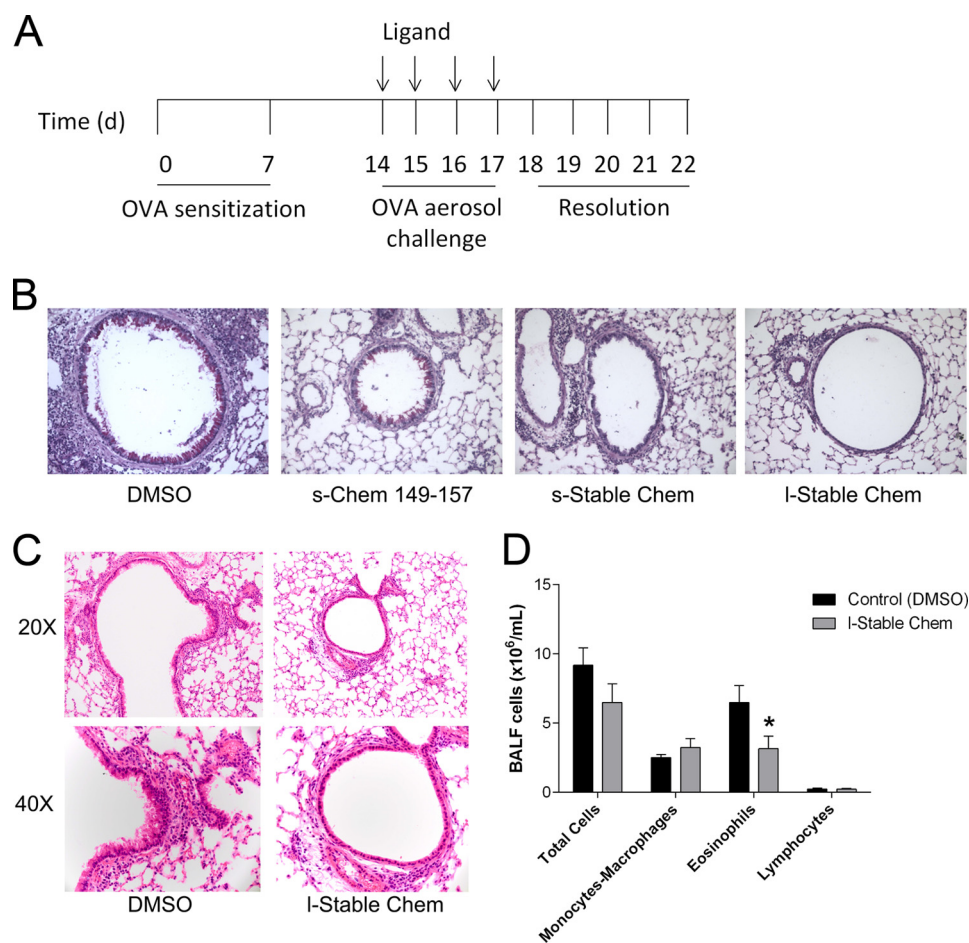
FIGURE 6. **l-Stable Chem dampens the development of allergic airway inflammation.** *A,* protocol for allergic airway inflammation: mice are sensitized with intraperitoneal OVA on days 0 and 7. Ligand is administered 30 min prior to challenge with aerosolized OVA on days 14–17. *B,* lung tissue sections from mice treated with DMSO, s-Chem(149–157), s-Stable Chem, or l-Stable Chem and sacrificed at day 18 were stained with periodic acid-Schiff reagent. Representative photographs are taken at ×20 magnification. *C,* lung tissue sections at day 18 were obtained from fixed, paraffin-embedded lung tissue stained with hematoxylin and eosin. Representative photographs are taken at both ×20 and 40. *D,* total BALF cells and leukocyte subsets were quantified on day 18 and compared between mice receiving DMSO or l-Stable Chem. Data are representative of the mean ± S.E. from $n = 3$–8 mice per group. Comparison of DMSO control to l-Stable Chem is shown: *, $p < 0.05$.

high potency at both the human and mouse CMKLR1 and anchored in the membrane as reflected by wash resistance. Given the *in vitro* efficacy of this compound at mouse CMKLR1, we pursued *in vivo* testing of this analog.

We utilized two distinct mouse disease models to assess the *in vivo* consequences of administering l-Stable Chem. In a model of allergic airway responses, the impact of s-Chem(149–157), s-Stable Chem, and l-Stable Chem were assessed. A hallmark feature of this model is mucus metaplasia in the airways. To varying extents, each of the 3 chemerin treatments resulted in decreased production of airway epithelial mucus. Notably, our data illustrate that the most pronounced decrease in periodic acid-Schiff reagent staining was observed with l-Stable Chem. These results establish that chemerin-based ligands can attenuate the mucus metaplasia that occurs as part of the allergic airway response.

At the same time, our results demonstrate that l-Stable Chem administration prior to OVA challenge in sensitized mice attenuates the development of lung inflammation (Fig. 6*C*). These anti-inflammatory effects were apparent both histologically and by a significant reduction in eosinophils quantitated in BALF. Because eosinophils are important mediators

in the pathophysiology of asthma, a decrease in these cells is likely to be protective both against tissue remodeling and airway dysfunction in this disease (36). Current therapeutics for asthma have in part targeted the biology of eosinophils by modulating their activity, chemotaxis, and survival (37). We believe that l-Stable Chem may be multipronged in its effect, providing both an anti-leukocyte effect as well as a protective effect against remodeling of the airway epithelium.

As a second index of *in vivo* efficacy, we examined the effects of l-Stable Chem on neuropathic pain following peripheral nerve injury. We illustrate that l-Stable Chem is effective at attenuating CCI-induced mechanical and cold hypersensitivity for at least 24 h post-administration supporting our postulate that this analog is long acting. In contrast to the prolonged duration of action of l-Stable Chem, RvE1 (also targeting CMKLR1) lost efficacy after 1 h, in agreement with a previous report in a comparable animal model (2). Even a stable analog of resolvin E1 (19-pf-RvE1), designed to resist local metabolic inactivation, only attenuates spinal nerve ligation-induced neuropathic pain for 6 h after injection (1). Taken together, these data suggest that l-Stable Chem may offer more prolonged
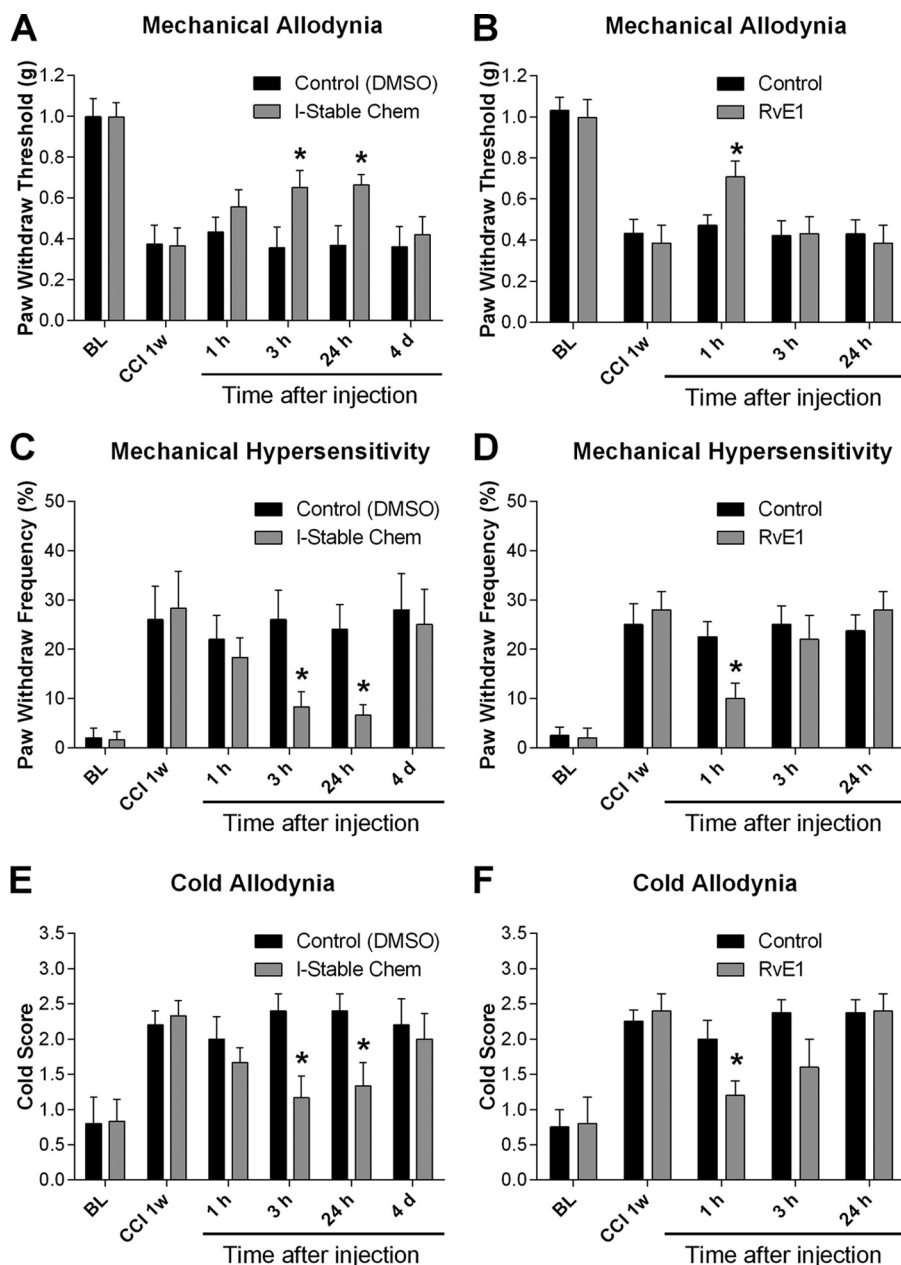
FIGURE 7. **Intrathecal treatment with l-Stable Chem reduces CCI-induced neuropathic pain.** Intrathecal injection of l-Stable Chem (100 pmol), 1 week after CCI, reduces CCI-induced mechanical hypersensitivity (*A* and *C*), and cold allodynia (*E*). Intrathecal injection of ResolvinE1 (*RvE1*) (100 pmol), 1 week after CCI, reduces CCI-induced mechanical hypersensitivity (*B* and *D*) and cold allodynia (*F*). *BL*, baseline before surgery. Data are representative of the mean ± S.E. from $n = 5$–8 mice per group. Comparison of control to l-Stable Chem or Resolvin-E1 is shown: *, $p < 0.05$.

analgesic effects and highlights the novelty and efficacy of this compound *in vivo*.

Although asthma and neuropathic pain manifest as distinct diseases, they fall under the broader category of inflammatory disorders. It is therefore possible that the therapeutic efficacy of l-Stable Chem observed in these two models share similar mechanisms. CMKLR1 is expressed on a variety of inflammatory cells, including: NK cells, DCs, and macrophages. Altered functional modulation of these cell types (*e.g.* chemotaxis, phagocytosis) may play a role in the mechanism of action of l-Stable Chem. Alternatively, direct interaction of l-Stable Chem on endothelial cells (asthma) or DRG/dorsal horn spinal cord neurons (4) may underlie the protective effects of this

ligand through the direct modulation of receptor-mediated signaling. Future studies aimed at further evaluating l-Stable Chem will reveal the cell-specific molecular mechanism underlying activity of this lipidated peptide.

Taken together, our data illustrate that l-Stable Chem is a potent inhibitor of allergic airway inflammation and neuropathic pain. The genesis of this compound and its efficacy *in vivo* will allow for dissection of pathways and evaluation of mechanisms of inflammation and synaptic transmission in disorders associated with CMKLR1 (ChemR23) signaling. In addition, given the putative role of the chemerin-CMKLR1 axis in other diseases (7, 38–40), it will be of interest to test l-Stable Chem in corresponding animal models. We anticipate, given

the success of this compound, that other GPCRs implicated in inflammation may be targeted using a similar approach. MTL technology as a predictive index for the pharmacological features of lipidated peptides provides a powerful strategy to develop novel compounds for the treatment of inflammatory disease.

REFERENCES

1. Ji, R. R., Xu, Z. Z., Strichartz, G., and Serhan, C. N. (2011) Emerging roles of resolvins in the resolution of inflammation and pain. *Trends Neurosci.* **34,** 599–609
2. Xu, Z. Z., Zhang, L., Liu, T., Park, J. Y., Berta, T., Yang, R., Serhan, C. N., and Ji, R. R. (2010) Resolvins RvE1 and RvD1 attenuate inflammatory pain via central and peripheral actions. *Nat. Med.* **16,** 592–597
3. Yoshimura, T., and Oppenheim, J. J. (2011) Chemokine-like receptor 1 (CMKLR1) and chemokine (C-C motif) receptor-like 2 (CCRL2): two multifunctional receptors with unusual properties. *Exp. Cell Res.* **317,** 674–684
4. Wittamer, V., Franssen, J. D., Vulcano, M., Mirjolet, J. F., Le Poul, E., Migeotte, I., Brézillon, S., Tyldesley, R., Blanpain, C., Detheux, M., Mantovani, A., Sozzani, S., Vassart, G., Parmentier, M., and Communi, D. (2003) Specific recruitment of antigen-presenting cells by chemerin, a novel processed ligand from human inflammatory fluids. *J. Exp. Med.* **198,** 977–985
5. Haworth, O., Cernadas, M., Yang, R., Serhan, C. N., and Levy, B. D. (2008) Resolvin E1 regulates interleukin 23, interferon-γ and lipoxin A4 to promote the resolution of allergic airway inflammation. *Nat. Immunol.* **9,** 873–879
6. Arita, M., Bianchini, F., Aliberti, J., Sher, A., Chiang, N., Hong, S., Yang, R., Petasis, N. A., and Serhan, C. N. (2005) Stereochemical assignment, anti-inflammatory properties, and receptor for the ω-3 lipid mediator resolvin E1. *J. Exp. Med.* **201,** 713–722
7. Bondue, B., Wittamer, V., and Parmentier, M. (2011) Chemerin and its receptors in leukocyte trafficking, inflammation and metabolism. *Cytokine Growth Factor Rev.* **22,** 331–338
8. Du, X. Y., and Leung, L. L. (2009) Proteolytic regulatory mechanism of chemerin bioactivity. *Acta Biochim. Biophys. Sin.* **41,** 973–979
9. Wittamer, V., Grégoire, F., Robberecht, P., Vassart, G., Communi, D., and Parmentier, M. (2004) The C-terminal nonapeptide of mature chemerin activates the chemerin receptor with low nanomolar potency. *J. Biol. Chem.* **279,** 9956–9962
10. Choi, C., Fortin, J. P., McCarthy, Ev., Oksman, L., Kopin, A. S., and Nitabach, M. N. (2009) Cellular dissection of circadian peptide signals with genetically encoded membrane-tethered ligands. *Curr. Biol.* **19,** 1167–1175
11. Fortin, J. P., Zhu, Y., Choi, C., Beinborn, M., Nitabach, M. N., and Kopin, A. S. (2009) Membrane-tethered ligands are effective probes for exploring class B1 G protein-coupled receptor function. *Proc. Natl. Acad. Sci. U.S.A.* **106,** 8049–8054
12. Harwood, B. N., Fortin, J. P., Gao, K., Chen, C., Beinborn, M., and Kopin, A. S. (2013) Membrane tethered bursicon constructs as heterodimeric modulators of the *Drosophila* G protein-coupled receptor rickets. *Mol. Pharmacol.* **83,** 814–821
13. Chou, K. C., and Elrod, D. W. (1999) Prediction of membrane protein types and subcellular locations. *Proteins* **34,** 137–153
14. Fortin, J. P., Chinnapen, D., Beinborn, M., Lencer, W., and Kopin, A. S. (2011) Discovery of dual-action membrane-anchored modulators of incretin receptors. *PLoS One* **6,** e24693
15. Cash, J. L., Hart, R., Russ, A., Dixon, J. P., Colledge, W. H., Doran, J., Hendrick, A. G., Carlton, M. B., and Greaves, D. R. (2008) Synthetic chemerin-derived peptides suppress inflammation through ChemR23. *J. Exp. Med.* **205,** 767–775
16. Schnölzer, M., Alewood, P., Jones, A., Alewood, D., and Kent, S. B. (1992) *In situ* neutralization in Boc-chemistry solid phase peptide synthesis: rapid, high yield assembly of difficult sequences. *Int. J. Pept. Protein Res.* **40,** 180–193
17. Pennington, M. W. (1994) HF cleavage and deprotection procedures for peptides synthesized using a Boc/Bzl strategy. *Methods Mol. Biol.* **35,** 41–62
18. Gill, S. C., and von Hippel, P. H. (1989) Calculation of protein extinction coefficients from amino acid sequence data. *Anal. Biochem.* **182,** 319–326
19. Doyle, J. R., Lane, J. M., Beinborn, M., and Kopin, A. S. (2013) Naturally occurring HCA1 missense mutations result in loss of function: potential impact on lipid deposition. *J. Lipid Res.* **54,** 823–830
20. Boussif, O., Lezoualc'h, F., Zanta, M. A., Mergny, M. D., Scherman, D., Demeneix, B., and Behr, J. P. (1995) A versatile vector for gene and oligonucleotide transfer into cells in culture and *in vivo*: polyethylenimine. *Proc. Natl. Acad. Sci. U.S.A.* **92,** 7297–7301
21. Conklin, B. R., Farfel, Z., Lustig, K. D., Julius, D., and Bourne, H. R. (1993) Substitution of three amino acids switches receptor specificity of $G\alpha_q$ to that of $G\alpha_i$. *Nature* **363,** 274–276
22. Kostenis, E., Martini, L., Ellis, J., Waldhoer, M., Heydorn, A., Rosenkilde, M. M., Norregaard, P. K., Jorgensen, R., Whistler, J. L., and Milligan, G. (2005) A highly conserved glycine within linker I and the extreme C terminus of G protein α subunits interact cooperatively in switching G protein-coupled receptor-to-effector specificity. *J. Pharmacol. Exp. Ther* **313,** 78–87
23. Summerhill, S., Stroud, T., Nagendra, R., Perros-Huguet, C., and Trevethick, M. (2008) A cell-based assay to assess the persistence of action of agonists acting at recombinant human β_2 adrenoceptors. *J. Pharmacol. Toxicol. Methods* **58,** 189–197
24. Romano, R., Dufresne, M., Prost, M. C., Bali, J. P., Bayerl, T. M., and Moroder, L. (1993) Peptide hormone-membrane interactions. Intervesicular transfer of lipophilic gastrin derivatives to artificial membranes and their bioactivities. *Biochim. Biophys. Acta* **1145,** 235–242
25. Bellucci, F., Carini, F., Catalani, C., Cucchi, P., Lecci, A., Meini, S., Patacchini, R., Quartara, L., Ricci, R., Tramontana, M., Giuliani, S., and Maggi, C. A. (2002) Pharmacological profile of the novel mammalian tachykinin, hemokinin 1. *Br. J. Pharmacol.* **135,** 266–274
26. Bennett, G. J., and Xie, Y. K. (1988) A peripheral mononeuropathy in rat that produces disorders of pain sensation like those seen in man. *Pain* **33,** 87–107
27. Xu, Z. Z., Liu, X. J., Berta, T., Park, C. K., Lu, N., Serhan, C. N., and Ji, R. R. (2013) Neuroprotectin/protectin D1 protects neuropathic pain in mice after nerve trauma. *Ann. Neurol.* **74,** 490–495
28. Xu, Z. Z., Berta, T., and Ji, R. R. (2013) Resolvin E1 inhibits neuropathic pain and spinal cord microglial activation following peripheral nerve injury. *J. Neuroimmune Pharmacol.* **8,** 37–41
29. Flatters, S. J., and Bennett, G. J. (2004) Ethosuximide reverses paclitaxel- and vincristine-induced painful peripheral neuropathy. *Pain* **109,** 150–161
30. Shimamura, K., Matsuda, M., Miyamoto, Y., Yoshimoto, R., Seo, T., and Tokita, S. (2009) Identification of a stable chemerin analog with potent activity toward ChemR23. *Peptides* **30,** 1529–1538
31. Luangsay, S., Wittamer, V., Bondue, B., De Henau, O., Rouger, L., Brait, M., Franssen, J. D., de Nadai, P., Huaux, F., and Parmentier, M. (2009) Mouse ChemR23 is expressed in dendritic cell subsets and macrophages, and mediates an anti-inflammatory activity of chemerin in a lung disease model. *J. Immunol.* **183,** 6489–6499
32. Zhang, L., and Bulaj, G. (2012) Converting peptides into drug leads by lipidation. *Curr. Med. Chem.* **19,** 1602–1618
33. Weinstock, M. T., Francis, J. N., Redman, J. S., and Kay, M. S. (2012) Protease-resistant peptide design-empowering nature's fragile warriors against HIV. *Biopolymers* **98,** 431–442
34. Powell, M. F., Stewart, T., Otvos, L., Jr., Urge, L., Gaeta, F. C., Sette, A., Arrhenius, T., Thomson, D., Soda, K., and Colon, S. M. (1993) Peptide

stability in drug development. II. Effect of single amino acid substitution and glycosylation on peptide reactivity in human serum. *Pharm. Res.* **10,** 1268–1273

35. Zhuang, Z. Y., Wen, Y. R., Zhang, D. R., Borsello, T., Bonny, C., Strichartz, G. R., Decosterd, I., and Ji, R. R. (2006) A peptide c-Jun N-terminal kinase (JNK) inhibitor blocks mechanical allodynia after spinal nerve ligation: respective roles of JNK activation in primary sensory neurons and spinal astrocytes for neuropathic pain development and maintenance. *J. Neurosci.* **26,** 3551–3560

36. Jacobsen, E. A., Ochkur, S. I., Lee, N. A., and Lee, J. J. (2007) Eosinophils and asthma. *Curr. Allergy Asthma Rep.* **7,** 18–26

37. Wegmann, M. (2011) Targeting eosinophil biology in asthma therapy. *Am. J. Respir. Cell Mol. Biol.* **45,** 667–674

38. Albanesi, C., Scarponi, C., Pallotta, S., Daniele, R., Bosisio, D., Madonna, S., Fortugno, P., Gonzalvo-Feo, S., Franssen, J. D., Parmentier, M., De Pità, O., Girolomoni, G., and Sozzani, S. (2009) Chemerin expression marks early psoriatic skin lesions and correlates with plasmacytoid dendritic cell recruitment. *J. Exp. Med.* **206,** 249–258

39. Ernst, M. C., and Sinal, C. J. (2010) Chemerin: at the crossroads of inflammation and obesity. *Trends Endocrinol. Metab.* **21,** 660–667

40. Ishida, T., Yoshida, M., Arita, M., Nishitani, Y., Nishiumi, S., Masuda, A., Mizuno, S., Takagawa, T., Morita, Y., Kutsumi, H., Inokuchi, H., Serhan, C. N., Blumberg, R. S., and Azuma, T. (2010) Resolvin E1, an endogenous lipid mediator derived from eicosapentaenoic acid, prevents dextran sulfate sodium-induced colitis. *Inflamm. Bowel Dis.* **16,** 87–95